Inelastic spin-exchange scattering of electrons from paramagnetic metals

G. A. Mulhollan, Xia Zhang, F. B. Dunning, and G. K. Walters
Department of Physics and the Rice Quantum Institute, Rice University, P.O. Box 1892, Houston, Texas 77251-1892
(Received 11 December 1989)

Spin-polarized electron-energy-loss spectra have been obtained from Cu(100) and Mo(110) surfaces by use of a polarized primary beam coupled with energy-resolved spin analysis of the scattered electrons. The data reveal strong evidence for inelastic spin-exchange scattering. In particular, a prominent polarization-loss feature evident in the Mo(110) data correlates with the joint density of states available for electron-hole pair excitation. Exchange scattering is observed to decrease rapidly with increasing primary beam energy.

Spin-polarized electron-energy-loss spectroscopy (SPEELS) has recently been employed to measure the electron-hole excitation spectra associated with the exchange-split d bands of the ferromagnetic $3d$ transition metals, and in particular to probe their Stoner densities of states.[1-6] In such experiments, the incident electron beam is polarized with spin parallel or antiparallel to the majority spin direction in the target, and the spin polarization of the scattered electrons is measured as a function of energy loss. The data are interpreted in terms of a scattering model based on electron-hole pair excitation that yields the rates for both spin-flip and non-spin-flip scattering.[2-4] Because of exchange splitting, both the spin-flip and non-spin-flip scattering rates for ferromagnets depend on whether the incident electrons are polarized parallel or antiparallel to the sample magnetization. A considerable simplification results when analyzing SPEELS data from a paramagnetic sample because, in the absence of exchange splitting, spin-flip and non-spin-flip scattering are each characterized by a single scattering rate, here denoted F and N, respectively.[6] In the present work, we explore the applicability of simple scattering models to the analysis of electron-hole excitation spectra from paramagnetic targets. Molybdenum and copper were selected for study because, as illustrated in Fig. 1(a), their densities of states are quite different from one another.[7] In particular, molybdenum, which has a high density of both occupied and unoccupied electronic states, is expected to exhibit strong inelastic scattering via electron-hole pair excitation, whereas in copper this process should be weak because there are so few unoccupied states.

The present apparatus is shown schematically in Fig. 2 and several of its component parts have been described in detail elsewhere.[8] Briefly, a collimated beam of spin-polarized electrons is directed at the target surface and the polarization of electrons scattered from the surface is measured as a function of energy and angle using a movable low-energy Mott polarimeter that is equipped with a retarding-potential energy analyzer. The polarized electron beam is produced by photoemission from a cesiated GaAs surface using circularly polarized radiation from a $Ga_{1-x}Al_xAs$ laser.[9] The photoelectrons, which are initially longitudinally polarized, are accelerated and directed through a 90° electrostatic deflector. The emergent beam, now transversely polarized, passes through a series of electrostatic lenses and is focused on the target surface. The polarization P_0 of the beam is ~ 0.26 and can be simply reversed, $\mathbf{P}_0 \rightarrow -\mathbf{P}_0$, by changing the sense of circular polarization of the radiation incident on the GaAs photocathode.

The Cu(100) and Mo(110) surfaces used in the present study were cleaned by repeated cycles of Ne^+ ion bombardment followed by thermal annealing. Surface cleanli-

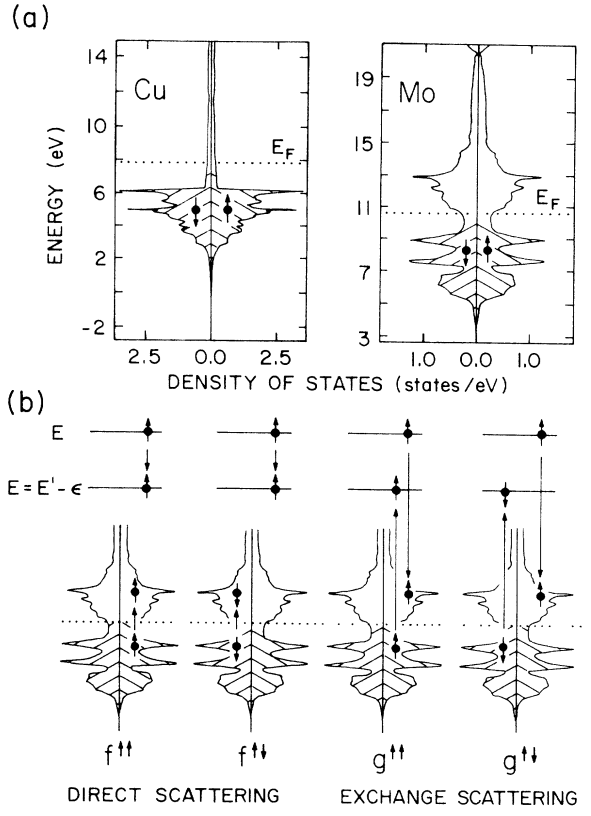

FIG. 1. (a) Densities of states for Cu and Mo (taken from Ref. 7); (b) schematic representation of the inelastic direct and exchange scattering channels important in the present work.

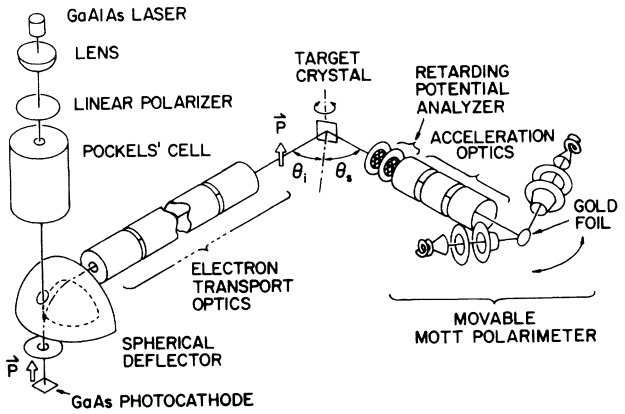

FIG. 2. Schematic diagram of the apparatus.

ness and order were monitored by Auger spectroscopy and low-energy electron diffraction (LEED), respectively.[10] Electrons leaving the target surface in a narrow range of angles ($\pm 5°$) about some angle θ_s to the surface normal enter a three-grid retarding-potential energy analyzer. The polarization of the incident electrons is perpendicular to the scattering plane defined by the incident electron beam and the axis of the energy analyzer. Those electrons with sufficient energy to overcome the retarding potential enter a low-energy Mott polarimeter where the average component of their spin polarization perpendicular to the scattering plane is determined by measuring the asymmetry that results due to the spin-orbit effect when the electrons are quasielastically scattered (at 15 keV) through $\pm 120°$ at a gold surface. The scattered electrons are detected by two symmetrically positioned channeltrons. The polarization of those electrons with energies between, say, $E-\Delta E/2$ and $E+\Delta E/2$ is determined by switching the potential applied to the retarding grids in the energy analyzer between the appropriate limits and measuring the asymmetry in the resulting *changes* in the count rates at each channeltron.

Rates for spin-flip and non-spin-flip inelastic scattering are derived from the measured asymmetries using a simple model[11] that assumes that the detected electrons emerge from the crystal following large-angle elastic scattering either preceded or followed by an inelastic electron-hole pair excitation event. The spin-flip and non-spin-flip scattering rates corresponding to an inelastic energy loss ε and momentum transfer $\mathbf{q}$ for, say, an incident spin-up ($\uparrow$) electron can be expressed in terms of the amplitudes for the direct and exchange scattering channels diagrammed in Fig. 1(b). In the case of direct scattering it is the incident electron that leaves the surface having suffered an inelastic energy loss, whereas for exchange scattering the emerging electron originates within the surface. The spin-flip and non-spin-flip scattering rates are given by

$$F=\sum|g_{\uparrow\downarrow}(\varepsilon,\mathbf{q})|^2 , \tag{1}$$

$$N=\sum[|f_{\uparrow\uparrow}(\varepsilon,\mathbf{q})-g_{\uparrow\uparrow}(\varepsilon,\mathbf{q})|^2+|f_{\uparrow\downarrow}(\varepsilon,\mathbf{q})|^2] , \tag{2}$$

where the summation is over states for which energy and momentum are conserved. Defining operators $\hat{F}$ and $\hat{N}$ associated with spin-flip and non-spin-flip scattering, respectively, we may write

$$\begin{aligned}\hat{F}|i^{\alpha}\rangle&=F|i^{-\alpha}\rangle ,\\ \hat{N}|i^{\alpha}\rangle&=N|i^{\alpha}\rangle ,\end{aligned} \tag{3}$$

where $\alpha=+$ or $-$ denotes spin-up ($|i^+\rangle$) or spin-down ($|i^-\rangle$) electrons. The possibility exists, however, that the operator $\hat{R}$ representing elastic scattering may also depend on the spin of the incident electron because of the spin-orbit effect. Thus if the operator $\hat{R}$ refers to the elastic scattering of spin-up and spin-down electrons we may write

$$\hat{R}|i^{\alpha}\rangle=R^{\alpha}|i^{\alpha}\rangle . \tag{4}$$

An incident electron beam of intensity I_0 and polarization βP_0, where $\beta=+$ or $-$ signifies an incident beam with spin up or spin down, respectively, may be decomposed as

$$|I_0\rangle=I_0^+|i^+\rangle+I_0^-|i^-\rangle , \tag{5}$$

where I_0^+ and I_0^- are the component spin-up and spin-down incident currents given by

$$I_0^{\pm}=I_0\left[\frac{1\pm\beta P_0}{2}\right] . \tag{6}$$

If such a beam is scattered from a target surface, then, remembering that electron-hole pair excitation can precede or follow large angle elastic scattering, the detected electron intensity is

$$\begin{aligned}|I\rangle&=I^+|i^+\rangle+I^-|i^-\rangle\\ &=[\hat{R}(\hat{N}+\hat{F})+(\hat{N}+\hat{F})\hat{R}][I_0^+|i^+\rangle+I_0^-|i^-\rangle] ,\end{aligned} \tag{7}$$

whereupon use of Eqs. (3) and (4) shows that the scattered spin-up (I^+) and spin-down (I^-) currents are

$$I^{\pm}(\beta)=\frac{I_0}{2}[2R^{\pm}N(1\pm\beta P_0)+(R^++R^-)F(1\mp\beta P_0)] . \tag{8}$$

Because of the spin-orbit effect, the scattered electron current may depend on the polarization of the incident beam and this dependence can be discussed using an asymmetry parameter A defined as

$$A=\frac{1}{P_0}\frac{[I^+(+)+I^-(+)]-[I^+(-)+I^-(-)]}{I^+(+)+I^-(+)+I^+(-)+I^-(-)} \tag{9}$$

which, with the aid of the expressions for $I^{\pm}(\beta)$ given in Eq. (8), may be written

$$A=\frac{N}{N+F}\frac{R^+-R^-}{R^++R^-} . \tag{10}$$

The polarization P^{β} of the scattered electrons for an incident beam polarization βP_0 is given by

$$P^{\beta}=\frac{I^+(\beta)-I^-(\beta)}{I^+(\beta)+I^-(\beta)} \tag{11}$$

which, again using Eq. (8), may be expressed as

$$P^{\beta}=\frac{A+\beta P_0\left[\frac{N-F}{N+F}\right]}{1+\beta P_0 A}, \tag{12}$$

where, in general, $P^{+}\neq -P^{-}$.

The asymmetry A is determined experimentally by measuring the change in the total detected current that results upon reversal of the polarization of the incident beam. It was found to be very small, $A\leq 0.05$, for all scattering conditions and energy intervals investigated in the present work, thus demonstrating that spin-orbit effects are quite small. This is not unexpected because the angular acceptance of the present analysis system is quite large ($\pm 5°$) and thus tends to average over any spin-orbit features that might be present (which are generally quite sharp in both angle and energy).

The polarization of the scattered electrons in some energy interval ΔE centered on the energy E is determined as follows. If the incident beam is initially polarized spin up ($\beta=+$), the count rates $R(E,\Delta E)$ in the two detection channels, labeled left and right, in the Mott polarimeter associated with scattered electrons having energies in the interval ΔE are related by

$$\frac{R_L(E,\Delta E)}{R_R(E,\Delta E)}=\left[\frac{1+SP^{+}(E,\Delta E)}{1-SP^{+}(E,\Delta E)}\right]\delta, \tag{13}$$

where $P^{+}(E,\Delta E)$ is given by Eq. (12), S is the magnitude of the effective Sherman function (~ 0.07), and δ is the instrumental asymmetry. Similarly, if the incident beam is polarized spin down ($\beta=-$), the ratio of the count rates becomes

$$\frac{R'_L(E,\Delta E)}{R'_R(E,\Delta E)}=\left[\frac{1+SP^{-}(E,\Delta E)}{1-SP^{-}(E,\Delta E)}\right]\delta. \tag{14}$$

These ratios are used to eliminate δ and define a measured polarization P_m as

$$P_m(E,\Delta E)=\frac{1}{S}\left[\frac{X-1}{X+1}\right], \tag{15}$$

where $X\equiv(R_L R'_R/R_R R'_L)^{1/2}$.[12]

Equations (12)–(15) can be used to relate P_m to the spin-flip and non-spin-flip scattering rates F and N, and to the known quantities S, P_0, and A. X may be written

$$X=\left[\frac{(1+SP^{+})}{(1-SP^{+})}\frac{(1-SP^{-})}{(1+SP^{-})}\right]^{1/2}\cong 1+S(P^{+}-P^{-}), \tag{16}$$

where, as justified below, higher-order terms are neglected. $P^{+}-P^{-}$ is given by

$$P^{+}-P^{-}=\frac{A+P_0 D}{1+P_0 A}-\frac{A-P_0 D}{1-P_0 A}=\frac{2P_0(D-A^2)}{1-P_0^2 A^2} \tag{17}$$

and

$$D\equiv\frac{N-F}{N+F}.$$

In the present experiments A is small ($\lesssim 0.05$) and, further, only enters Eq. (17) in second order. Thus, to a good approximation we may write $P^{+}-P^{-}\cong 2P_0 D$ whereupon, combining Eqs. (15) and (16), P_m may be expressed as

$$P_m=\frac{1}{S}\left[\frac{SP_0 D}{1+SP_0 D}\right]. \tag{18}$$

Equation (18) can be further simplified [and the neglect of higher-order terms in Eq. (16) justified] because in the present work S ($\cong 0.07$) and P_0 ($\cong 0.26$) are both small. Thus

$$P_m\cong P_0 D=P_0\left[\frac{N-F}{N+F}\right]. \tag{19}$$

Use of this expression allows fractional rates for spin-flip and non-spin-flip scattering to be extracted from the measured polarizations P_m and these are given by

$$\frac{F}{N+F}=\frac{1}{2}\left[1-\frac{P_m}{P_0}\right],\qquad \frac{N}{N+F}=\frac{1}{2}\left[1+\frac{P_m}{P_0}\right]. \tag{20}$$

The measured polarization P_m of electrons scattered from both Mo(110) and Cu(100) surfaces (normalized to unit incident electron polarization) is shown in Fig. 3 as a function of scattered electron energy. These data were obtained under specular geometry ($\theta_i=\theta_s=55°$) with an

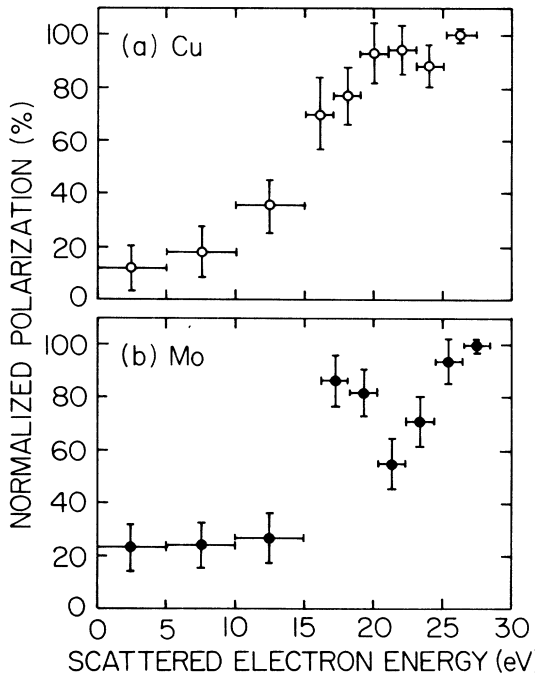

FIG. 3. The measured polarizations P_m of electrons scattered from (a) Cu(100) and (b) Mo(110) surfaces as a function of scattered electron energy. The data are normalized to unit incident electron polarization and were obtained under specular geometry ($\theta_i=\theta_s=55°$). The incident electron energy is 26 eV and the energy interval ΔE is 2 eV.

incident electron energy of 26 eV. The energy interval ΔE is 2 eV. For Mo(110) a pronounced local minimum in the measured electron polarization is observed at energies corresponding to an inelastic energy loss of ~ 6 eV. This same feature was also present in Mo(110) data acquired under nonspecular conditions ($\theta_i = 55°$, $\theta_s = 70°$), and with different incident electron energies. The size of the feature, however, decreased with increasing incident electron energy. This is illustrated in Fig. 4 which shows the average polarization of those scattered electrons that have suffered inelastic energy losses of between 4 and 6 eV as a function of incident electron energy. No local minimum in the measured electron polarization was detected in any of the Cu(100) data.

Fractional rates for spin-flip and non-spin-flip scattering obtained from the data in Fig. 3 by use of Eq. (20) are displayed in Fig. 5 for inelastic energy losses ε of up to 10 eV. For larger values of ε, secondary electrons provide an increasing contribution to the total detected electron signal, as evidenced by the onset of a rapid increase in the scattered electron current and concurrent decrease in the average electron polarization. In this regime, the present model, which assumes that the scattered electrons simply comprise inelastically scattered primary electrons, is no longer applicable. Nonetheless, the fact that, for Mo(110), the scattered electron polarization is large for energy losses ε of ~ 10 eV suggests that inelastic electron-hole pair excitation is the major source of the detected electrons. The maximum in the spin-flip scattering rate for Mo at $\varepsilon \sim 6$ eV is clearly evident.

As suggested by Fig. 1(b), the importance of spin-flip exchange scattering depends on the densities of both occupied and unoccupied states. In the approximation that the transition matrix elements coupling occupied and unoccupied states are independent of energy and constant over the Brillouin zone, the spin-flip scattering rate for some inelastic energy loss ε, $F(\varepsilon)$, may be written

$$F(\varepsilon) \propto \int_{E_F-\varepsilon}^{E_F} n_0(E) n_u(E+\varepsilon) dE \ , \tag{21}$$

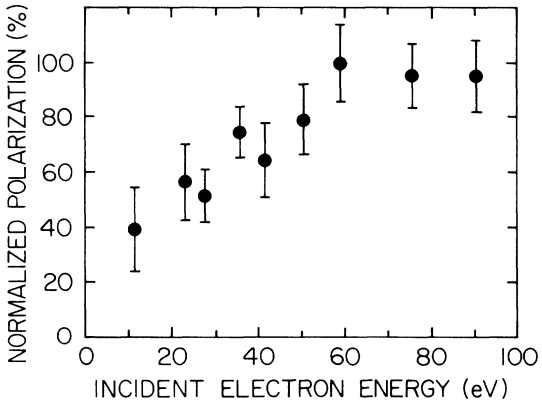

FIG. 4. Measured average polarization of electrons scattered from Mo(110) that have suffered inelastic energy losses between 4 and 6 eV as a function of incident electron energy. The data are normalized to unit incident electron polarization and were recorded under specular geometry ($\theta_i = \theta_s = 55°$).

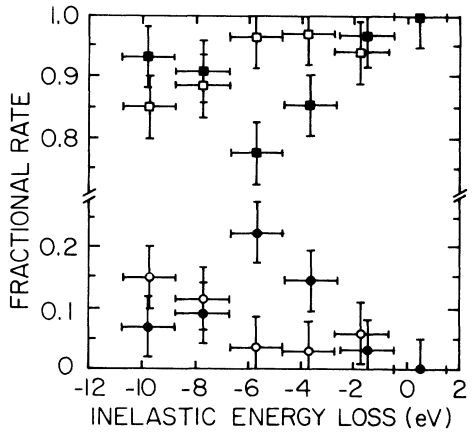

FIG. 5. Fractional rates for spin-flip (F) and non-spin-flip (N) scattering as a function of inelastic energy loss ε. Spin-flip scattering: Mo, ⊢•⊣ ; Cu, ⊢○⊣ . Non-spin-flip scattering: Mo, ⊢•⊣ ; Cu, ⊢○⊣ .

i.e., $F(\varepsilon)$ is proportional to the convoluted density of occupied (n_o) and unoccupied (n_u) states.[13] Values of $F(\varepsilon)$ obtained in this manner for both Mo and Cu are presented in Fig. 6 together with the experimental data. The calculated $F(\varepsilon)$ are normalized to the experimental data at an inelastic energy loss $\varepsilon \sim 6$ eV. (The normalization constants for Mo and Cu are not substantially different, suggesting that their averaged transition matrix elements are comparable.) The agreement between experiment and calculation is quite satisfactory suggesting that the two-particle exchange scattering model is valid, even for rather sizeable inelastic energy losses. The decrease in the size of the Mo(110) spin-flip scattering feature with increasing electron energy apparent in Fig. 4 is also consistent with exchange scattering because the overlap of the electron wave functions decreases at higher energies, i.e., when the velocity of the incident electron greatly exceeds the Fermi velocity, it is distinguishable from electrons in the Fermi sea and exchange processes should be

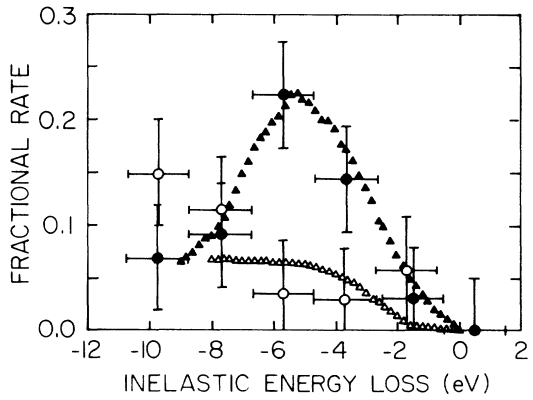

FIG. 6. Fractional rates for spin-flip scattering as a function of inelastic energy loss ε. Experimental data: Mo, ⊢•⊣ ; Cu, ⊢○⊣ . Calculation: Mo, ▲▲▲; Cu, △△△.

suppressed.[14]

To the extent that transition matrix elements do not vary greatly from target to target, simple joint-density-of-states arguments suggest that spin-flip-scattering effects might be expected to be small when s-p electrons (which provide only a low density of unoccupied states) dominate the band structure near the Fermi level. Indeed, Hopster has demonstrated that graphite shows little evidence of spin-flip scattering.[11] Preliminary investigations in this laboratory suggest that this is also true for GaAs surfaces. In addition, in their early work on spin-exchange mean free paths, Hüfner *et al.*[15] reported that there was no evidence of spin-flip scattering from a thick layer of potassium. Hence, it appears that only in systems with high densities of states both above and below the Fermi level, such as afforded by the *nd* transition metals, are spin-flip scattering processes easily observable. We also note that, based on the simple joint-density-of-state analysis presented here, SPEELS spectra from paramagnetic Fe, Co, and Ni are expected to exhibit significant structure over the same ranges of energy loss as those for which Stoner excitations are important in scattering from the corresponding ferromagnetic targets.[1-5] Finally, the good agreement between experiment and the predictions of the simple two-particle scattering model described here suggests that electron-hole pair excitation is the predominant inelastic electron scattering mechanism for energy losses of up to ~ 10 eV, at least for Mo and Cu surfaces. Further work along the present lines will provide a valuable test of theoretical treatments of electron-hole pair excitation.[13,14,16]

We wish to thank Professor A. Ignatiev for the loan of the Mo(110) crystal. This research is supported by the Division of Materials Sciences, Office of Basic Energy Sciences of U.S. Department of Energy, and by the Robert A. Welch Foundation (Houston, TX).

[1]J. Kirschner, D. Rebenstorff, and H. Ibach, Phys. Rev. Lett. **53**, 698 (1984).

[2]A. Venus and J. Kirschner, Phys. Rev. B **37**, 2199 (1988); J. Kirschner, Phys. Rev. Lett. **55**, 973 (1985).

[3]H. Hopster, R. Raue, and R. Clauberg, Phys. Rev. Lett. **53**, 695 (1984).

[4]D. L. Abraham and H. Hopster, Phys. Rev. Lett. **62**, 1157 (1989); H. Hopster and D. L. Abraham, Phys. Rev. B **40**, 7054 (1989).

[5]Y. U. Izerda, D. A. Papaconstanpoulos, G. A Prinz, B. T. Jonker, and J. J. Krebs, Phys. Rev. Lett. **61**, 1222 (1988).

[6]S. Yin and E. Tosatti, International Center for Theoretical Physics, Trieste, Report No. IC/81/129 (1981) (unpublished).

[7]D. A. Papaconstanpoulos, *Handbook of the Band Structure of Elemental Solids* (Plenum, New York, 1986).

[8]G. A. Mulhollan, X. Zhang, F. B. Dunning, and G. K. Walters, Phys. Rev. B **39**, 8715 (1989); F.-C. Tang, X. Zhang, F. B. Dunning, and G. K. Walters, Rev. Sci. Instrum. **59**, 504 (1988).

[9]D. T. Pierce, R. J. Celotta, G.-C. Wang, W. N. Unertl, A. Galejs, C. E. Kuyatt, and S. R. Mielczarek, Rev. Sci. Instrum. **51**, 478 (1980).

[10]Although the Cu surface could be completely cleaned by sputtering and annealing, approximately one-tenth of a monolayer of C remained on the Mo surface. Tests revealed, however, that the SPEELS data were insensitive to carbon coverage up to the monolayer level.

[11]H. Hopster, D. L. Abraham, and D. P. Pappas, J. Appl. Phys. **64**, 5927 (1988). However, the procedure used here for introducing the parameters $R^{\pm}$ differs from that proposed by Hopster *et al.* The predictions of the two models, nonetheless, agree in the limit that $A \sim 0$, i.e., $R^{+} \cong R^{-}$.

[12]$P_m = |P^{\beta}|$ when $A = 0$. See L. A. Hodge, J. T. Moravec, F. B. Dunning, and G. K. Walters, Rev. Sci. Instrum. **50**, 5 (1979).

[13]D. R. Penn, S. P. Apell, and S. M. Girvin, Phys. Rev. B **32**, 7753 (1985).

[14]S. Modesti, F. Della Valle, C. J. Bocchetta, E. Tosatti, and G. Paolucci, Phys. Rev. B **36**, 4503 (1987); S. Modesti, F. Della Valle, R. Rosei, E. Tosatti, and J. Glazer, *ibid.* **31**, 5741 (1985).

[15]S. Hüfner, G. L. Bora, F. Meier, and D. Pescia, Solid State Commun. **51**, 1631 (1984).

[16]D. R. Penn and S. P. Apell, Phys. Rev. B **38**, 5051 (1988); D. R. Penn, *ibid.* **35**, 1910 (1987).